

pubs.acs.org/accounts Article

Function and Aggregation in Structural Eye Lens Crystallins

Kyle W. Roskamp, Carolyn N. Paulson, William D. Brubaker, and Rachel W. Martin*



ACCESS Metrics & More Soluble Insoluble aggregates

CONSPECTUS: Crystallins are transparent, refractive proteins that contribute to the focusing power of the vertebrate eye lens. These proteins are extremely soluble and resist aggregation for decades, even under crowded conditions. Crystallins have evolved to avoid strong interprotein interactions and have unusual hydration properties. Crystallin aggregation resulting from mutation, damage, or aging can lead to cataract, a disease state characterized by opacity of the lens.

Different aggregation mechanisms can occur, following multiple pathways and leading to aggregates with varied morphologies. Studies of variant proteins found in individuals with childhood-onset cataract have provided insight into the molecular factors underlying crystallin stability and solubility. Modulation of exposed hydrophobic surface is critical, as is preventing specific intermolecular interactions that could provide nucleation sites for aggregation. Biophysical measurements and structural biology techniques are beginning to provide a detailed picture of how crystallins crowd into the lens, providing high refractivity while avoiding excessively tight binding that would lead to aggregation.

Despite the central biological importance of refractivity, relatively few experimental measurements have been made for lens crystallins. Our work and that of others have shown that hydration is important to the high refractive index of crystallin proteins, as are interactions between pairs of aromatic residues and potentially other specific structural features.

This Account describes our efforts to understand both the functional and disease states of vertebrate eye lens crystallins, particularly the γ -crystallins. We use a variety of biophysical techniques, notably NMR spectroscopy, to investigate crystallin stability and solubility. In the first section, we describe efforts to understand the relative stability and aggregation propensity of different γ S-crystallin variants. The second section focuses on interactions of these proteins with the holdase chaperone α B-crystallin. The third, fourth, and fifth sections explore different modes of aggregation available to crystallin proteins, and the final section highlights the importance of refractive index and the sometimes conflicting demands of selection for refractivity and solubility.

■ INTRODUCTION

The crystallins of the vertebrate eye lens are structural proteins that maintain the transparency and high refractive index of the lens, enabling it to focus light on the retina. Because of the unique functional requirements of this tissue, the fiber cells elongate and lose their organelles during development. The resulting mature fiber cells contain exceptionally high concentrations of crystallin proteins, comprising nearly 90% of the dry weight of the human lens. Lens crystallins must function throughout an organism's lifetime, despite frequent exposure to UV light, which can cause irreversible and deleterious photochemistry. As demonstrated by King and

co-workers, the ability of $\beta\gamma$ -crystallins to resist photoinduced damage depends on two highly conserved pairs of Trp residues, one in each domain.² Mutating these key Trp residues to Phe reduces the UV absorption of these proteins but greatly increases their aggregation propensity upon UV

Received: January 14, 2020 Published: April 9, 2020





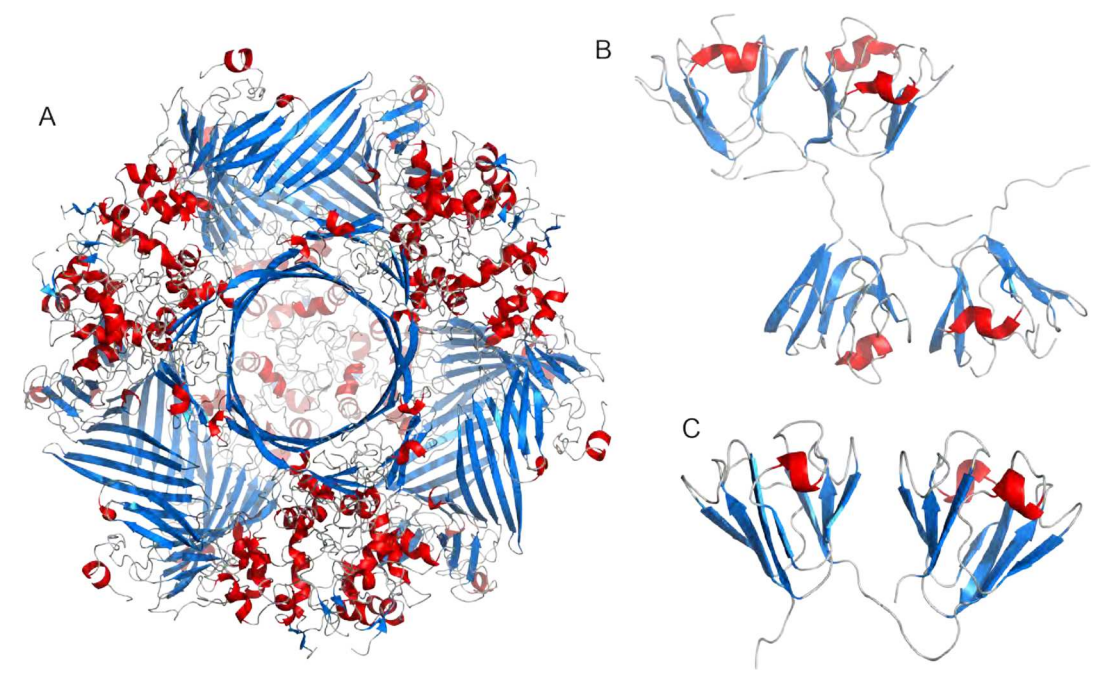


Figure 1. Representative structures of the three major crystallin types in the vertebrate eye lens. (A) Human αB-crystallin multimer (PDB ID 2YGD).¹³ (B) Bovine βB1-crystallin dimer (PDB ID 1BLB).¹⁴ (C) Homology model of monomeric human γS-crystallin based on the murine structure (PDB ID 1ZWO).¹⁵

irradiation.³ The effect is especially pronounced for mutation of the more strongly quenched Trp residues, suggesting a photoprotective quenching mechanism involving multiple tryptophans.⁴ Under UV irradiation, Trp residues can also undergo photochemistry to produce products such as kynurenine, which provide additional UV filtering in the lens⁵ but can accelerate oxidative damage when covalently attached to crystallin proteins.⁶ In addition to their obvious biomedical relevance, the extraordinary biophysical properties of the lens crystallins make them a fertile ground for investigating the fundamentals of protein solubility and aggregation. Many studies in this topic space have focused on particularly aggregation-prone proteins, but understanding these phenomena also requires detailed studies of proteins that resist aggregation, even under difficult conditions.

In contrast to most proteins, which have turnover half-lives as short as minutes for ornithine decarboxylase⁷ or up to a month for some immunoglobulins,8 the crystallins are not replaced after their initial expression during early development because of the loss of organelles in the lens fiber cells. This extraordinary longevity places lens crystallins, along with most other proteins in the lens,⁹ in a unique class known as extremely long-lived proteins (ELLPs). Other well-known examples are collagen and elastin, the structural proteins of the extracellular matrix, which form a cross-linked polymeric structure, and the scaffold proteins of the nuclear pore complex, which exist within massive cellular machinery structures. 10 Compared with other ELLPs, the lens α - and β crystallin oligomers are relatively small, while the γ -crystallins are monomeric. In the crowded lens fiber cells, crystallincrystallin interactions are critical for maintaining solubility, as relatively few types of proteins are present. Surprisingly, the attractive interactions of the γ -crystallins¹¹ do not lead to aggregation despite their high concentration, longevity, negligible protein turnover, and frequent exposure to damaging UV radiation. The failure of this system causes crystallin aggregation, which is central to the etiology of cataract, the leading cause of blindness worldwide and a World Health Organization priority eye disease. 12

Vertebrate lens crystallins belong to two major families, α and $\beta \gamma$. The two are grouped together on the basis of their common function rather than structural similarity, as they have different folds and separate evolutionary histories. Representative structures of each type are shown in Figure 1. The α crystallins (Figure 1A) are small heat shock proteins that function as holdase chaperones, which bind to damaged structural proteins but lack ATPase activity and therefore cannot refold them. In addition to the lens, they are expressed in several different tissues, including heart, brain, and kidney. 16 Structurally, α -crystallins are composed of mostly unstructured N- and C-terminal domains flanking a 90-residue immunoglobulin-like α -crystallin domain. Monomers come together to form hetero- and homodimers, which serve as the building blocks for high-molecular-weight complexes. These complexes are dynamic and heterogeneous, with the most common species ranging in size from 24-mers to 33-mers. $^{13,17-19}$ αA -Crystallins form smaller oligomers assembled from tetrameric subunits, with associations mediated by cross-dimer domain swapping. Unlike α B-crystallin, which has no cysteines, this protein can transfer disulfide bonds to aggregation-prone client proteins to help keep them in solution,²⁰ a role that is complementary to the function of glutathione as the primary redox buffer of the lens. Binding interactions with both α Aand αB -crystallin can also proceed via contact of exposed hydrophobic surfaces on the client protein with specific regions of the chaperone. Subsequent analysis and characterization of these α -crystallin peptide sequences, named mini- α A/Bcrystallin (M α AC/M α BC), have shown that they retain chaperone activity in vitro. 21

The lens β - and γ -crystallins have evolved from an ancestral Ca²⁺-binding protein. ²² Members of this family are characterized by the $\beta\gamma$ -crystallin domain, a β -sandwich composed of

a double Greek key motif containing four antiparallel strands within each sheet. A conserved feature of the $\beta\gamma$ -crystallin superfamily is a (F/Y/W)-x-x-x-(F/Y)-x-G sequence found across the first β -hairpin of each Greek key. The aromatic side chains in this motif participate in π -stacking interactions, while the glycine is capable of adopting unconventional backbone torsion angles. Lens β - and γ -crystallins have in common two characteristic $\beta\gamma$ -crystallin domains, but there are several important differences as well: β -crystallins (Figure 1B) are typically dimeric and have longer interdomain linkers and Nand C-terminal extensions than the more compact, monomeric γ -crystallins (Figure 1C). Both the structure of the $\beta\gamma$ -crystallin fold and the two-domain architecture of the structural lens crystallins are important for their stability. Hydrophobic residues are almost exclusively packed into the core of the β sandwich in each domain and at the interdomain interface. Externally, the γ-crystallin surface is a patchwork of acidic, basic, and neutral polar residues that form a highly interconnected network of hydrogen bonds and salt bridges. Interspersed internally and externally are pairs and collections of aromatic residues that form $\pi - \pi$ -stacking interactions. Systematic removal of key residues has shown that each contributes to protein stability but that modifications of Nterminal residues result in greater destabilization than the equivalent C-terminal domain mutations.²³ The two domains are structurally very similar, though they are not identical in sequence; the interdomain interface is also critical for maintaining stability.²⁴

This Account focuses on our efforts to understand the molecular factors underlying the extraordinary stability and solubility of the crystallin proteins. We have used a variety of biophysical techniques to elucidate the molecular determinants of human crystallin solubility and aggregation.

IDENTIFYING KEY SEQUENCE DETERMINANTS OF γS-CRYSTALLIN STABILITY

One way to separate the effects of folding and intermolecular interactions on protein aggregation is to investigate variant proteins with reduced solubility or stability. Surprisingly, many crystallin mutations causing autosomal dominant cataract result in proteins that are fully folded at room temperature but have reduced thermal stability and aggregate at physiological temperatures, either alone or in mixed precipitates with one or more α -crystallins. These known mutations provide a clear starting point; however, it is essential to test hypotheses about the molecular basis of protein solubility using site-directed mutagenesis.

We began by studying the G18V variant (γ S-G18V), on the basis of its role in childhood-onset cataract, ²⁵ and the replacement of a highly conserved glycine in a tight turn with a bulky hydrophobic residue. We then designed the symmetry-related variant γ S-G106V, which occupies the homologous position in the C-terminal domain, in order to determine whether the increased aggregation propensity is due to the G to V mutation per se or structural factors specific to the N-terminal domain. This comparison would elucidate whether the reduced solubility of G18V is due to gross misfolding, altered intermolecular interactions due to exposure of a previously buried hydrophobic residue, or more subtle structural effects necessitating further characterization.

Our experimental results and molecular dynamics simulations performed by our collaborators demonstrated that these two superficially similar mutations have quite different effects

on folding stability and solubility.²⁶ At room temperature, comparison of the circular dichroism (CD) spectra of wildtype γ S-crystallin (γ S-WT), γ S-G18V, and γ S-G106V indicated that all three are folded, with a primarily β -sheet secondary structure. However, interesting differences became apparent upon heating. Although both variants are less stable than γS-WT, \gammaS-G106V is substantially less stable than the diseaserelated \(\gamma \)S-G18V. Monitoring the aggregates that form using dynamic light scattering (DLS) gave the opposite result: γS-G18V is by far the more aggregation-prone variant. This result was somewhat surprising because in many discussions of protein misfolding and aggregation, a decrease in thermodynamic stability is used as a proxy for increased aggregation propensity. Along the way to structure determination, NMR chemical shifts indicated that γ S-G18V has significant conformational differences in much of the N-terminal domain, 27 whereas the effects of γ S-G106V are limited to the area directly surrounding the mutation site (Figure 2).²⁸ An increase in conformational flexibility was also recently observed for aggregation-prone γS-crystallin variants mimicking deamidation in age-related cataract.²⁹

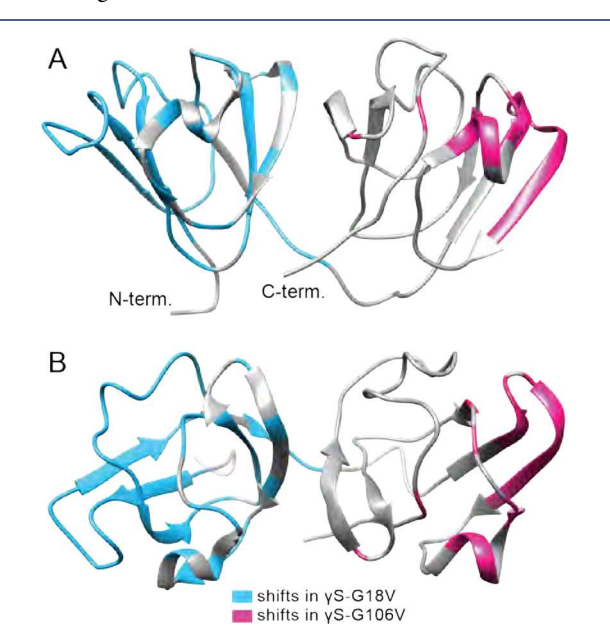


Figure 2. (A) "Front" and (B) "top" views of γS-WT (PDB ID 2M3T), indicating that the residues that have significantly different chemical shifts in γS-G18V (light blue) and γS-G106V (magenta) relative to γS-WT. NMR chemical shift perturbations are a sensitive probe of the local chemical environment and hence serve as a reporter for local changes in conformation. Adapted from ref 28. Copyright 2013 American Chemical Society.

Contrary to initial hypotheses, the solution NMR structures of γ S-WT and γ S-G18V (Figure 3A) revealed that the first 17 residues of γ S-G18V are largely unaffected by the mutation. V18, at odds with the molecular dynamics simulations, the original hypotheses, and conventional wisdom regarding backbone torsion angles, remains in almost the same position as G18 in γ S-WT (Figure 3B). Instead of being exposed to solvent, the V18 side chain remains buried, wedged tightly between two β -strands. As a result, the amide proton of R19 is locked between the V18 terminal methyl groups, avoiding A-1,3 strain and resulting in a drastic difference in the dihedral angles of R19 relative to the wild type (Figure 3C). This 180°

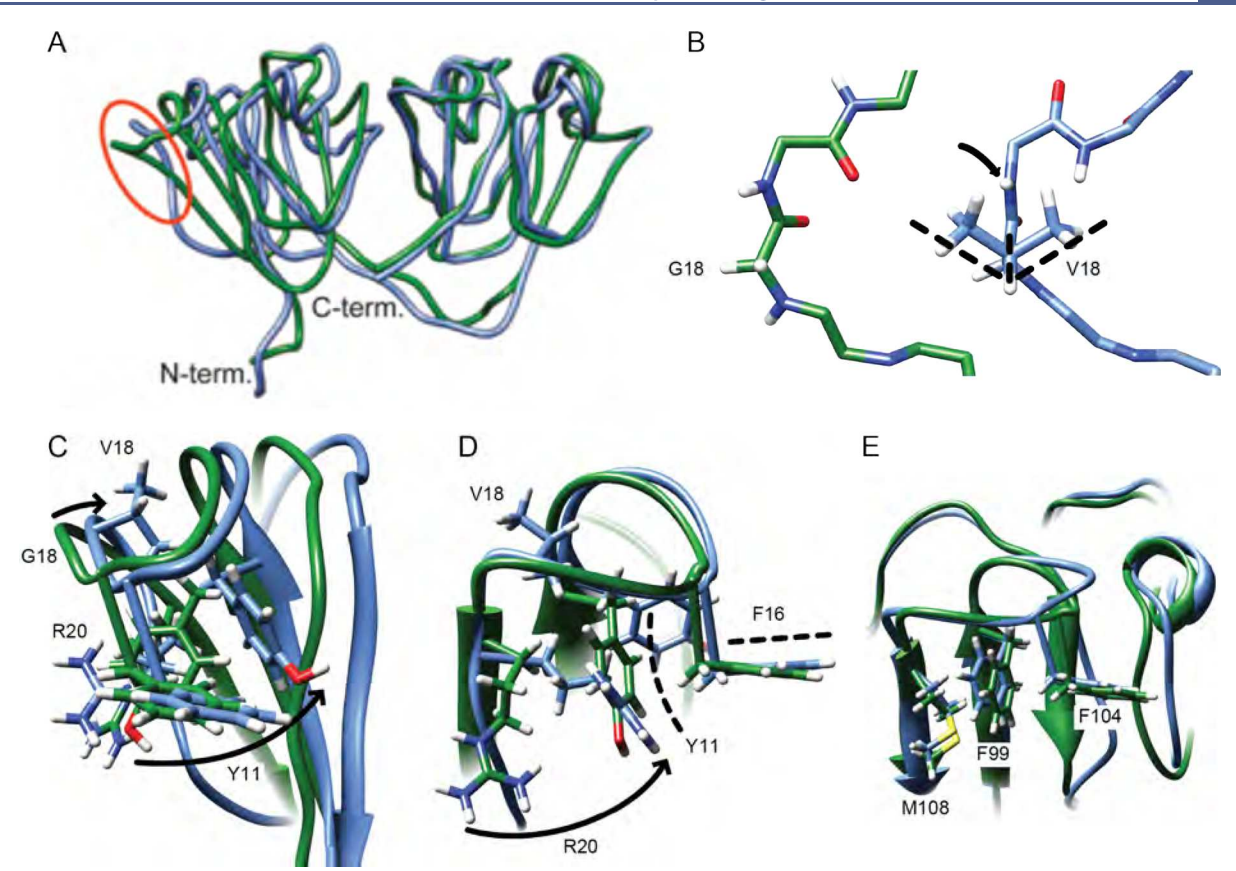


Figure 3. Ribbon diagrams showing the structural differences between γS-WT (green) and γS-G18V (blue). (A) Overlay of the two structures. (B) The backbone near the mutation site undergoes subtle structural changes. In γS-G18V, the backbone dihedral angles for residue 18 occupy a disallowed region for non-glycine residues. In γS-WT, the G18 torsion angles are $\phi = 73.7$, $\psi = 163.0$, while for V18 in γS-G18V they are $\phi = 129.8$, $\psi = 134.3$. (C) The addition of V18 and its effect on the backbone angles the β -strand outward. The torsion angles of R20 shift from $\phi = -58.6^{\circ}$, $\psi = -177.2^{\circ}$ in γS-WT to $\phi = -110.2^{\circ}$, $\psi = -17.9^{\circ}$ in γS-G18V. (D) R20 displaces Y11 and forces the phenol ring away from F16 and against the β -strands. Here R20 appears to also adopt the same highly conserved perpendicular ring orientation with F16 that Y11 occupies in γS-WT, possibly forming a stabilizing interaction. (E) C-terminal outer corner loop region of γS-WT and γS-G18V. F99, F104, and M108 side chains are shown. M108 lacks a planar side-chain group to replace F99 in the perpendicular ring motif, making a similar stabilizing rearrangement impossible in γS-G106V. Panels A–D adapted with permission from ref 30. Copyright 2013 Cell Press.

rotation of the ψ angle of R19 of γS-G18V disrupts the R20-C23 β -strand, causing a conformational change that is propagated throughout the backbone of the N-terminal domain. In γ S-G18V, the R20 C β is rotated inward, which in turn displaces Y11. In γ S-WT, this residue participates in an edge-face π -stacking interaction with F16. In γ S-G18V, the planar guanidinium group from R20 replaces the ring of Y11 in a π -stacking interaction stabilizing the first β -strand and corner loop (3D). This stabilizing rearrangement is not available to γS-G106V: the three corresponding residues in the C-terminal domain are F99, F104, and M108 (Figure 3E). M108 is unable to participate in a similar stability-enhancing π -stacking interaction because it lacks a planar side-chain group containing delocalized π electrons. This suggests that the outer corner loop of the C-terminal domain is disrupted as a result of the G106V mutation, leading to a hypothesis about why γ S-G106V is thermally less stable than both γ S-WT and γS-G18V.

Additional variants (γ S-G18V/R20A, γ S-G18V/R20M, and γ S-G106V/M108R) were constructed to test our hypotheses about how structural factors affect stability. CD and DLS measurements were performed as in our previous studies of γ S-crystallin variants. Table 1 summarizes the midpoint temperatures of unfolding ($T_{\rm m}$) for all of the variants studied;

Table 1. Thermal Unfolding Temperatures for γ S-Crystallin Variants

protein variant	T_{m} (°C)
γS-WT	72.0 ± 0.1
γ S-G18V	63.6 ± 0.1
γS-G106V	58.9 ± 0.1
γ S-G18V/R20A	67.1 ± 0.1
γ S-G18V/R20M	63.1 ± 0.1
γS-G106V/M108R	62.7 ± 0.1

the thermal unfolding curves are shown in Figure 4A,B. The M108R substitution confers stability to γ S-G106V as expected: the $T_{\rm m}$ of γ S-G106V/M108R is 62.7 °C, which is several degrees higher than that of γ S-G106V and similar to that of γ S-G18V. Unexpectedly, the substitution of R20 with alanine increases the stability of γ S-G18V, while substituting it with methionine has little effect on the stability. Although substituting M108 with arginine does restore the thermal stability of γ S-G106V to the same level as γ S-G18V, the data for the variants with mutations in the N-terminal domain suggest that R20 does not confer stability to the N-terminal domain of γ S-G18V in the manner hypothesized above: when it is removed, the resulting structures are not destabilized.

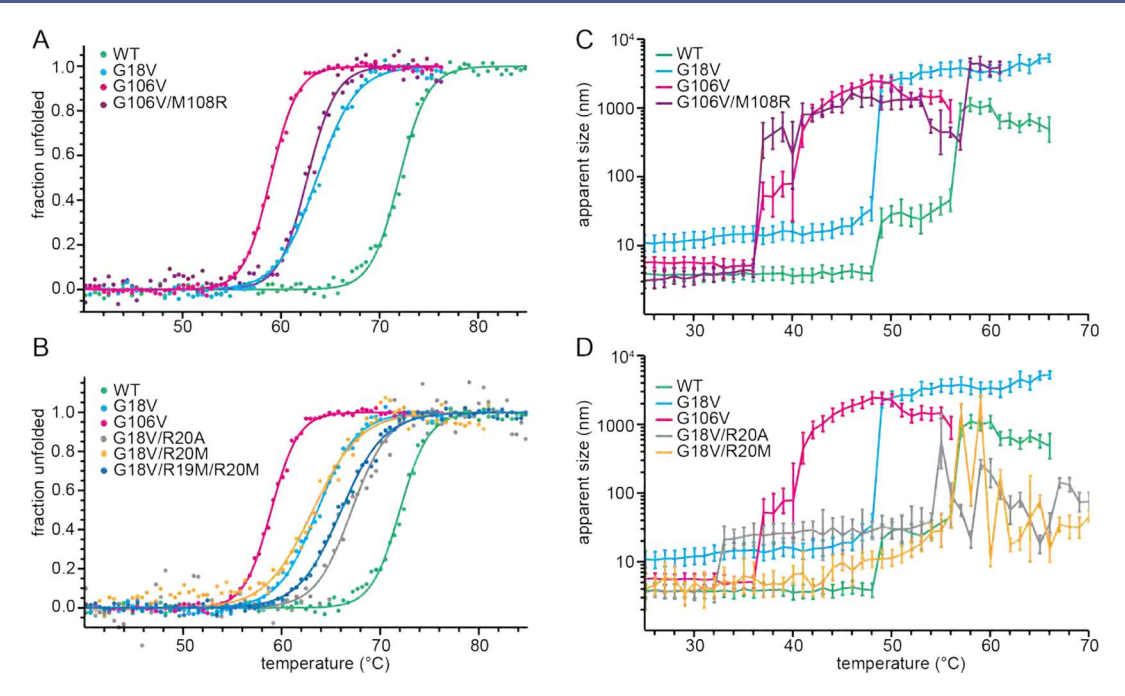


Figure 4. (A) Thermal unfolding data for variants of human γS-crystallin: γS-WT (green), γS-G18V (light blue), γS-G106V (magenta), and γS-G106V/M108R (purple). Unfolding was measured by monitoring the CD signal at 218 nm; lines are best-fit unfolding curves. Replacing M108 with R accounts for nearly the entire stability difference between γS-G18V and γS-G106V. (B) Thermal unfolding data for γS-WT (green), γS-G18V (light blue), γS-G106V (magenta), γS-G18V/R20A (orange), γS-G18V/R20M (gray), and γS-G18V/R19M/R20M (dark blue). Contra the initial hypothesis, replacing R20 with M has little effect on the stability, while replacing R20 with A or R19 and R20 with M increases the stability relative to γS-G18V. (C) Thermal aggregation measured using DLS for the γS-crystallin variants described in (A). As previously described, G18V is the most aggregation-prone. The aggregation propensity of γS-G106V/M108R is higher than that of γS-G106V; their aggregation onset temperatures are similar, but γS-G106V/M108R forms larger aggregates. (D) DLS measurements during thermal aggregation for the γS-crystallin variants described in (B). Overall, these data illustrate that the relationship between thermal stability and aggregation propensity is not easily predictable.

To gauge the effects these mutations have on the aggregation propensity of γ S-crystallin, the formation of thermally induced aggregates was also monitored by DLS, and the results are shown in Figure 4C,D. In contrast to the stability results, the M108R mutation of γ S-G106V increases the overall aggregation propensity of the protein. In γ S-G106V, intermediate-sized aggregates are formed at 36 °C, whereas γ S-G106V/M108R instead forms large aggregates directly. Unlike γ S-G18V, which often forms oligomers below 30 °C, both γ S-G18V/R20A and γ S-G18V/R20M begin as monomers at 25 °C. At 32 °C, γ S-G18V/R20A forms intermediate-sized aggregates before developing much larger aggregates at 54 °C. γ S-G18V/R20M gradually forms intermediate aggregates near 42 °C that grow rapidly beginning at 56 °C.

Overall, observation of the thermal denaturation of these γ Scrystallin variants does not support the hypothesis that R20 provides extra stability to the N-terminal domain of γ S-G18V: when the functionality of R20 was removed, the resulting variants experienced an increase in thermal stability. However, as in the initial set of experiments, the aggregation propensity of these \(\gamma \)-crystallin variants does not follow the same trend as their thermal stabilities. Replacing R20 with either A or M decreases the aggregation propensity of \(\gamma \)S-G18V, whereas replacing M108 with R in the corner loop of the C-terminal domain of γ S-G106V leads to the elimination of intermediate aggregate formation in favor of larger aggregates of γS-G106V/ M108R at a higher temperature. It appears that while R20 participates in a favorable interaction, it also locks the Nterminal domain of γ S-G18V in a conformation that promotes self-aggregation. These results support the idea that aggregation propensity is not correlated to thermal stability in a straightforward manner.

Instead, we hypothesize that a major driver of roomtemperature aggregation in \(\gamma S-G18V \) appears to be the solvent exposure of the previously buried residues C23, C25, and C27 (Figure 5), which allows the formation of intermolecular disulfides as a starting point for aggregation. This is consistent with observations in the literature for both γ S- and γ Dcrystallin: intramolecular disulfide bonding apparently traps the W42R and W42Q variants of \(\gamma \text{D-crystallin} \) in a partially misfolded conformation that promotes aggregation,³ intermolecular disulfide bond formation is essential for dimer formation in γ S-WT.³² In γ S-G18V, this type of disulfide bonding may be facilitated by the increased exposure of C23, C25, and C27 relative to their positions in γ S-WT. Of course, dimerization is only the first step in aggregation, and detailed solid-state NMR measurements, such as those performed for the native-like aggregates of $\gamma D\text{-P23T}$, 33 are needed to elucidate the structural basis for the disease state.

RECOGNITION OF AGGREGATION-PRONE CLIENTS BY THE HOLDASE CHAPERONE αB-CRYSTALLIN

Point mutations are frequently assumed to have only a very local effect on protein structure; our work and that of other groups have indicated that this is often not the case for crystallins.³⁵ As discussed in the previous section, the relatively minor conformational change caused by the G18V mutation nevertheless propagates down the polypeptide chain through more than half of the N-terminal domain.³⁰ In collaboration

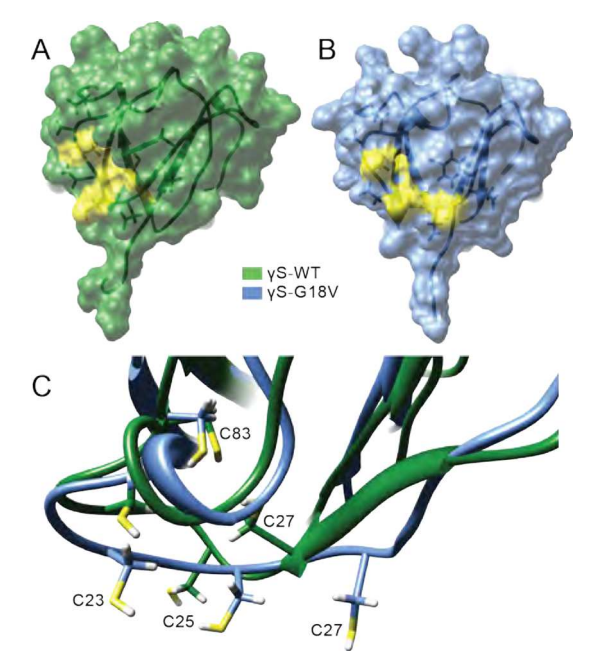


Figure 5. Molecular surfaces of (A) γS-WT (PDB ID 2M3T) and (B) γS-G18V (PDB ID 2M3U)³⁴ showing the exposure of additional cysteines C23, C25, and C27 (yellow) in γS-G18V. (C) Overlaid ribbon structures of γS-WT (green) and γS-G18V (blue), showing the positions of the relevant cysteine side chains.

with Oschkinat and co-workers, we performed solution-state NMR experiments to identify the particular surface of G18V that interacts with the molecular chaperone α B-crystallin. This protein binds to misfolded structural crystallins in the lens and keeps them in solution but is unable to refold them. In this role, it binds only weakly and transiently to wild-type γ S, even under heat stress (Figure 6A,B). In contrast, it binds γ S-G18V strongly and specifically (Figure 6C,D). To characterize the interactions between αB and γS , heteronuclear single-quantum coherence (HSQC) spectroscopy was performed on mixtures of ¹⁵N-labeled γS-WT and γS-G18V with natural-abundance α B. Because NMR spectroscopy is sensitive to small changes in the electronic environment of the detected nuclei, binding interactions between αB and γS result in shifts or disappearances of relevant cross-peaks representing specific N-H moieties, providing exquisitely specific information about the interaction in solution. To our knowledge, this was the first binding interface between \(\alpha \)B-crystallin and an aggregation-prone structural crystallin to be characterized.

We also directly probed the exposed hydrophobic surface on γ S-G18V that is recognized by α B-crystallin. In a concerted experimental and computational study performed with the Tobias group, we explored the binding of γ S-WT and γ S-G18V to the fluorescent dye 8-anilinonaphthalene-1-sulfonic acid (ANS). Binding of this dye, measured via an increase in fluorescence intensity relative to the unbound state, serves as an imperfect but useful proxy for exposed hydrophobic surface area. Although ANS fluorescence provides quantitative information about hydrophobic surface exposure, it lacks molecular-level detail. Therefore, we investigated specific binding sites using NMR chemical shift perturbations and docking simulations performed by Tobias and co-workers, yielding a detailed picture of how the dye interacts with the protein. We then tied these results back to α -crystallin binding by demonstrating that ANS competitively interferes with the

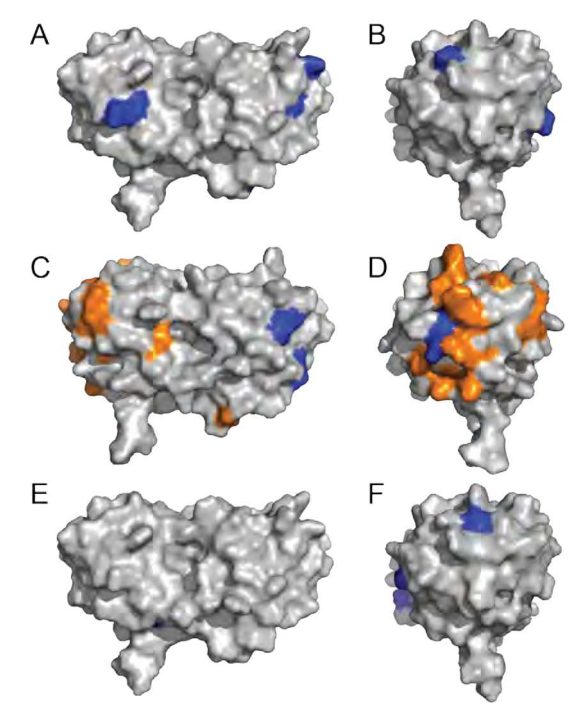


Figure 6. Surfaces of γ S-WT colored to show residues involved in interactions with α B-crystallin, as measured by solution-state NMR spectroscopy. Two views are shown: (A) "front" and (B) with the N-terminal domain rotated forward. Noninteracting residues are shown in gray, while those involved in weak, transient interactions are shown in blue. (C) and (D) show the same views of γ S-G18V with noninteracting residues in gray, weakly interacting residues in blue, and strongly interacting residues in orange. (E) and (F) show the same views of γ S-G18A with noninteracting and weakly interacting residues shown using the same color coding. Panels A–D adapted with permission from ref 30. Copyright 2013 Cell Press. Panels E and F generated from data reported by Sprague-Piercy et al. ³⁶

αΒ-γS-G18V interaction.³⁷ In contrast to the results for γS-G18V, replacing G18 with alanine produces a much smaller, more local structural perturbation that does not produce a substantial increase in exposed hydrophobic surface area. The γS-G18A variant has decreased thermal stability and increased aggregation propensity relative to γS-WT, albeit to a lesser extent than γS-G18V. We initially hypothesized that a protein of intermediate aggregation propensity between γS-WT and γS-G18V would also recruit αB-crystallin, although perhaps with lower affinity than the disease-related variant. However, this was not the case for γS-G18A, which αB-crystallin does not bind (Figure 6E,F). This result indicates that αB-crystallin is able to distinguish among structurally similar variants of its client proteins.³⁶

Taken together, these results suggest that the intermolecular interactions of α B-crystallin are precisely tuned to bind only aggregation-prone variants of its client proteins. This is consistent with a view of cataractogenesis in which the finite allotment of α -crystallin in the lens is used up by damaged or mutated structural crystallins; the highly aggregation-prone γ S-G18V variant occupies a lifetime's worth of binding capacity in a few short years, causing childhood-onset cataract. Cataract disease progression may also be accelerated by the large complexes formed between human α B-crystallin and its client proteins, particularly if exposed hydrophobic areas are incompletely protected. These mixed crystallin particles may be more prone to aggregation and precipitation as a result of

exposure of aggregation-prone regions on their surfaces, an idea that we call the "sticky side out" hypothesis. To date, the exact mechanism of aggregation in the lens is not fully understood, but it appears likely that in the case of severely aggregation-prone structural crystallin variants, holdase chaperone activity may result in recruitment of ever-larger amounts of α B-crystallin to the complexes, eventually exhausting the holdase chaperone capability of the lens.

■ INTERACTIONS OF HUMAN EYE LENS PROTEINS WITH SOLVENT

Dehydration is thought to play an important role in protein aggregation, disrupting solvent-solute interactions and causing irreversible interprotein interactions. Despite the importance of such interactions, there is a dearth of mechanistic detail on the relationship between the binding of water at the protein surface and initiation of aggregation. One important set of questions relates to the relative importance of environmental factors versus characteristics of the protein itself. Are protein surface dehydration and subsequent aggregation effects that occurs as a function of crowding, confinement, and pressure, or is the aggregation propensity actually dictated by the hydration shell, whose stability and compressibility are intrinsic properties of the protein surface? In collaboration with Han and coworkers, we found the latter to be the case: wild-type human γ S-crystallin harbors a dynamic yet exceptionally stable hydration shell. In contrast, in γ S-G18V this stability is greatly altered, suggesting that maintaining a robust, mobile water layer is essential to maintaining the extraordinary solubility of γ S-WT. Indeed, a critical function of γ S-crystallin in the eye lens may be precisely its capacity to preserve this stable hydration shell.

Our study showed that upon crowding of γ S-WT, the population of the stable surface hydration water is increased, but no new water population with slower dynamics or otherwise altered properties is generated. Using a combination of Overhauser dynamic nuclear polarization (ODNP) and solution-state NMR spectroscopy, we directly observed the link between the stability of this protein's hydration shell and its aggregation propensity. The Han lab has pioneered ODNP methods for observing the relaxation behavior and hence the mobility of water near the protein surface. Here, ODNP experiments showed that the hydration water of γ S-WT retains its rapid bulklike mobility up to extremely high protein concentrations (greater than 500 mg/mL), while that of γ S-G18V dramatically and irreversibly slows down at much lower protein concentrations, as is typical for most proteins.

In order to gain detailed molecular-level insight into this phenomenon, we measured the amide temperature coefficients, which directly report on site-specific protein-solvent interactions. Because hydrogen bonding, either intramolecular or to the solvent, greatly influences the local electronic environment of amide protons, the temperature dependence of the ¹H chemical shifts reveals whether the amide proton of a given residue participates in intramolecular hydrogen bonding. For globular proteins, the temperature coefficients of the backbone resonances are usually linear over a temperature range up to about 15 K below the thermal denaturation temperature. Typical values range from -16 to +2 ppb/K. Below the denaturation temperature, increasing the temperature increases the magnitudes of local fluctuations in the protein structure, causing lengthening of each hydrogen bond and hence movement of the chemical shift toward its random coil

value. At the mutation site (residue 18), there is a large difference in chemical shift, but the difference in chemical shift as a function of temperature, $\delta \Delta/\Delta T$, for G18 of γ S-WT (-4.98 ppb/K) versus V18 of γ S-G18V (-3.00 ppb/K) is relatively subtle, indicating that V18 is involved in an intermolecular hydrogen bond, consistent with our NMR structures. Our analysis revealed that several other residues in the N-terminal domain do have a different hydrogen-bonding status in γ S-WT than in γ S-G18V. Overall, the cataract-related variant has more hydrogen bonds to solvent than γ S-WT, underscoring the point that increasing protein—water interactions does not necessarily lead to greater solubility: greater solvent interaction with normally buried hydrophobic groups can lead to fragility of the hydration shell and hence aggregation.

The observations that aggregation-prone γS-G18V has altered interactions with water and α B-crystallin led us to investigate the character of the particular aggregates formed. A variety of aggregation mechanisms have been proposed, with experimental evidence supporting each. Given the different cataract phenotypes and genetic and environmental factors as well as by analogy to other protein condensation diseases, it is likely that cataractogenesis can occur through a variety of pathways. Some researchers have observed the presence of fibrillar aggregates similar to those seen in Alzheimer's, Huntington's, and Parkinson's diseases, 40 while others have reported amorphous-looking aggregates in which the monomers retain native-like structure.33 Our observations of the aggregation of γS-WT and γS-G18V driven by pH extremes, high temperatures, and UV exposure also indicate multiple pathways leading to different products: all of the aggregation conditions tested produced a mixture of aggregate types. Both low and high pH favored amyloid fibrils, while amorphous aggregates were the dominant species in heat-treated and UV-exposed samples.⁴¹ Other researchers have observed a variety of aggregation mechanisms in structural crystallins, including disulfide-induced dimerization, ³² domain swapping, ^{42,43} loss of key interactions in the interdomain interface, 44 partial 45 or complete⁴⁶ unfolding of the N-terminal domain, and bridging via metal chelation.47

■ METAL ION BINDING AND AGGREGATION

In addition to mutation and oxidative or photochemical damage, crystallin aggregation can also be caused by interactions with other species in the lens, including metal ions. Metal-ion-induced aggregation is particularly interesting in light of the evolutionary origin of the vertebrate lens $\beta\gamma$ crystallins. These proteins evolved from an ancestral protein similar to the Ca²⁺-binding $\beta\gamma$ -crystallin from the tunicate *Ciona intestinalis* (*Ci-\beta\gamma*). Tunicates are believed to have diverged from cerebrates before the development of the eye. In metal-ion-binding crystallins, including several from microbial species and Ci- $\beta\gamma$, binding of divalent cations is essential for maintaining protein stability. Ci- $\beta\gamma$ contains a double-clamp Ca²⁺-binding motif, which is characterized by the sequence D/ N-N/D-X-X-S/T-S, and is typical of microbial $\beta\gamma$ crystallins. 50 We determined that Ci- $\beta\gamma$ binds Ca^{2+} with very high affinity ($K_d \approx 0.05 \mu M$), resulting in very high thermal and chemical stability: the Ca2+-bound form tolerates temper-

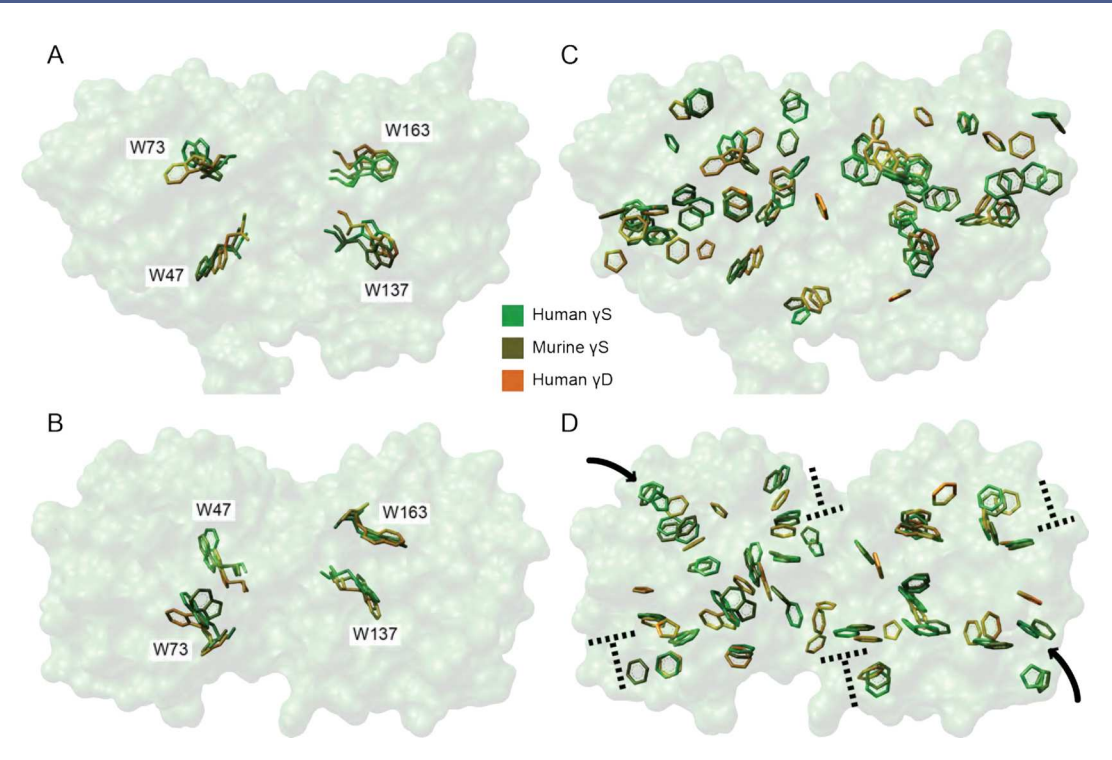


Figure 7. Molecular surfaces of human γS- (green), murine γS- (khaki, PDB ID $2A5M^{59}$), and human γD-crystallins (orange, PDB ID $2KLJ^{60}$), with aromatic residues highlighted. (A) "Front" and (B) "top" views showing the positioning of the four conserved tryptophans. W47 and W163 occupy very similar orientations in all three structures, W73 is highly variable, and the indole ring of W137 is flipped in the structure of human γS. (C) "Front" and (D) "top" views showing all of the aromatic residues. A perpendicular ring motif is consistent across all of the corner loops (dotted lines), and ring stacking in the outer bottom loops is also fairly consistent across the three structures (arrows).

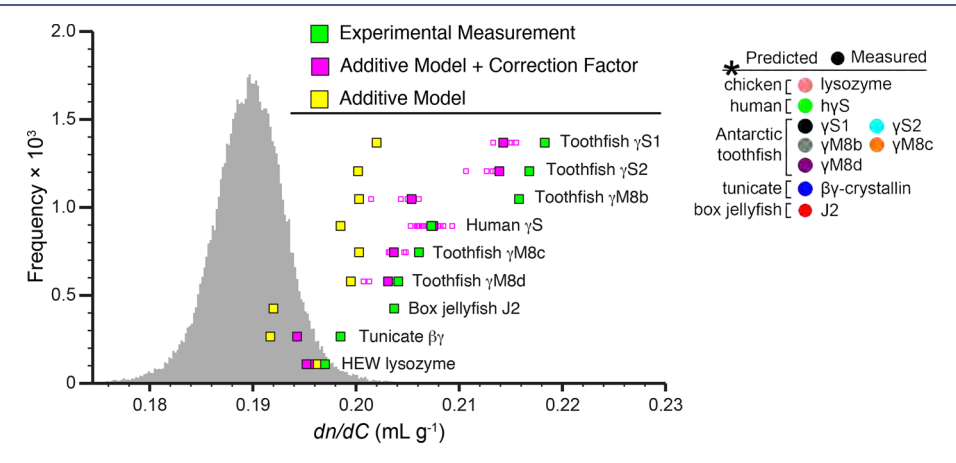


Figure 8. Predicted and measured dn/dc values for toothfish γS1-, γS2-, γM8b-, γM8c-, and γM8d-crystallins, hen egg white (HEW) lysozyme, human γS-crystallin, box jelly J2-crystallin, and tunicate βγ-crystallin. Experimentally measured (green), additive Gladstone–Dale model predictions (yellow), and predictions using the π-pair correction (magenta) are shown for each protein. The histogram depicts the predicted dn/dc values for the human proteome generated using the additive model (gray). In cases where multiple conformations are available, e.g., human γS-crystallin, corrected predictions are shown with solid squares for the lowest-energy structure and open squares for alternate conformations. For HEW lysozyme, two solid squares representing two crystal structures are shown, while no predictions are shown for J2-crystallin, which lacks known homologues that could be used for homology modeling.

atures up to 94 °C and 8 M urea, in contrast to the much less stable apo form. Stable apo form. We identified specific cation-binding residues using NMR chemical shift perturbations. The first time, we observed binding of Ci- $\beta\gamma$ to several other divalent cations, with varying effects on its stability.

In contrast, vertebrate lens crystallins lack this feature and bind Ca²⁺ only weakly and nonspecifically if at all: many of them have positively charged residues at key positions, abrogating cation binding. Some researchers have suggested that the loss of Ca²⁺-binding affinity was required for the

vertebrate crystallins to evolve their high refractivity, ⁵³ while others have observed that some human β - and γ -crystallins have weak Ca²⁺ binding activity. ^{54,55} We did not observe any changes to the structure or solubility of human γ S-crystallin upon addition of Ca^{2+,51} whereas other divalent cations promote aggregation. ⁵²

■ REFRACTIVE INDEX

Most studies of structural crystallins to date have focused on their extraordinary stability and solubility, which are indeed

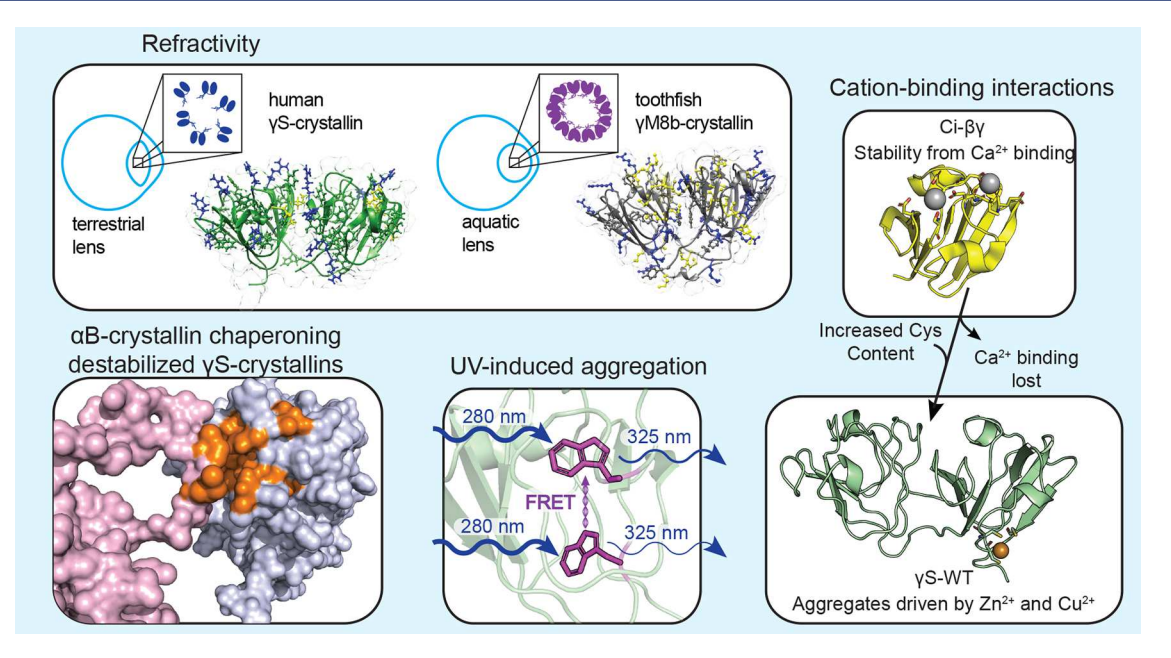


Figure 9. Summary of the major themes related to βγ-crystallins discussed in this Account. Clockwise from top left: Aquatic lenses are more refractive than terrestrial ones because of the shape of the lens, the protein concentration, and the refractivity of the crystallins themselves (illustrated here by highlighting highly refractive residues, including aromatics, arginines, and methionines.) Divalent cations stabilize tunicate βγ-crystallin, which resembles microbial cation-binding crystallins, but either do not bind or do not cause aggregation in human γS-crystallin. UV light causes chemical modification of tryptophan residues, as observed by other researchers, including King and Truscott. We observe that UV-induced aggregates are similar to those induced by thermal denaturation rather than those produced by extreme pH conditions. We observe that human αB-crystallin recognizes aggregation-prone variants of human γS-crystallin that have significant differences in hydrophobic surface area but not those with only minor and local structural disruption. Overall, the structural and refractive functions of the βγ-crystallins are sometimes in tension, providing a fascinating system for investigating the biophysical chemistry of protein stability.

critical to their function in the lens. However, they are also strongly selected for high refractivity, which entails a high concentration of polarizable amino acids and is sometimes at odds with selection for solubility. This effect is particularly pronounced in the lenses of aquatic organisms, which do not derive focusing power from an air-water interface at the cornea, leading to much more stringent selection for refractivity. The refractive index is defined as the ratio of the velocity of light in a vacuum to its velocity in a given isotropic medium. When traversing between media, the extent to which light is bent is a function of the refractive index, which can be readily determined using Snell's law. The contribution to the change in refractive index with concentration for proteins is known as the refractive index increment (dn/dc). A conventional value of 0.185 is often used for all proteins, as relatively few dn/dc values have been experimentally measured. A more refined model estimates the dn/dc value on the basis of sequence. However, our experimental dn/dc measurements on recombinant γ -crystallins show that such additive models substantially underestimate the refractivity of lens proteins, particularly those from aquatic animals.

We performed the first measurements of the refractive index increment for seven crystallins from aquatic organisms: tunicate Ci- $\beta\gamma$ -crystallin, Antarctic toothfish γ S1-, γ S2-, γ M8b-, γ M8c-, and γ M8d-crystallins, and box jelly J2-crystallin. All of the measured values were much higher than their predicted ones. We found that the factors correlating most strongly with anomalous dn/dc values were exposure of hydroxyl groups on the protein surface and pairs of highly polarizable amino acids with π systems in close proximity, a feature that is common in lens crystallins (Figure 7). The latter observation led to our π -pair correction to the additive model

of dn/dc, yielding better agreement with experimental results.⁵⁷ Figure 8 shows a comparison between experimentally measured dn/dc values and those calculated using the additive model alone as well as with the π -pair correction, which accounts for much of the discrepancy between the additive model and the experimental data. Another potential source of error in the additive model is failure to account for the protein's hydration shell, which is quite different from that of a solution of its component amino acids. Intriguingly, zebrafish γM-crystallins have been observed to have very weak interactions with water, ⁵⁸ consistent with our own observations of the hydration shell of human γS-crystallin.³⁹ We observed that the Dissostichus mawsoni yM-crystallins predicted by molecular modeling to have the most exposed hydroxyl groups also have the greatest deviations in dn/dc from the additive model, suggesting that the unusual hydration behavior of γ crystallins is important for their core refractive function as well as avoiding aggregation. Solving the structures of these proteins and investigating their hydration shells in detail will allow us to begin to disentangle the complex relationships among surface hydration, solubility, and refractivity.

SUMMARY AND OUTLOOK

Crystallins are a unique class of ELLPs that remain soluble and transparent for the life of the organism, even in the absence of protein turnover and under frequent UV light exposure. Numerous mutations and post-translational modifications are known to impact crystallin solubility, but the molecular-level details of the aggregation process and sometimes even the aggregates formed are highly variable. Our work on crystallin aggregation focuses on using a variety of biophysical techniques in order to explore as many aspects of the

phenomenon as possible. In order to fully understand crystallin stability, solubility, and transparency, more experimental data are required to inform generalizations about the underlying molecular properties. In particular, more structures of aggregation-prone variants, both disease-related and engineered to test specific hypotheses, are needed, as well as solid-state NMR and cryo-EM structures of the disease-related aggregates. Another exciting direction is the structural and biophysical study of fish crystallins, which have evolved to withstand temperature and pressure extremes as well as concentrations even higher than those found in the human lens. Experimental measurements of protein refractivity and intermolecular interactions are also essential for elucidating the physical chemistry underlying lens function. Lessons learned from studies of these fascinating aggregation-resistant proteins will not only guide future cataract treatments and improve the design of artificial lenses but also be broadly applicable to understanding protein solubility and aggregation more generally. Figure 9 summarizes the major themes of our work on $\beta\gamma$ -crystallins.

AUTHOR INFORMATION

Corresponding Author

Rachel W. Martin — Department of Chemistry and Department of Molecular Biology and Biochemistry, University of California, Irvine, California 92697-2025, United States; Occid.org/0000-0001-9996-7411; Email: rachel.martin@uci.edu

Authors

Kyle W. Roskamp — Department of Chemistry, University of California, Irvine, California 92697-2025, United States

Carolyn N. Paulson — Institute for Therapeutics Discovery and Development, University of Minnesota, Minneapolis, Minnesota 55414, United States; orcid.org/0000-0001-8564-7345

William D. Brubaker — SRI International, Menlo Park, California 94025, United States

Complete contact information is available at: https://pubs.acs.org/10.1021/acs.accounts.0c00014

Notes

The authors declare no competing financial interest.

Biographies

Kyle W. Roskamp is a recent Ph.D. graduate of the University of California, Irvine. He received his Bachelor of Arts from Pomona College, double majoring in Chemistry and Mathematics. At UC Irvine he worked with Prof. Rachel Martin to investigate the protein aggregation pathways of the γ -crystallins. He also worked to characterize the evolutionary adaptations of γ -crystallins for functionality in the lens.

Carolyn N. Paulson is a research scientist in the Institute for Therapeutics Discovery and Development at the University of Minnesota. She earned her Bachelor of Science in Biochemistry at UCLA and her Ph.D in Chemistry at UC Irvine. At UC Irvine, she worked with Prof. Rachel Martin to study intermolecular interactions between eye lens crystallins using solution-state NMR spectroscopy and other biophysical techniques. She did her postdoctoral research at the University of Illinois at Chicago with Prof. Michael Caffrey, where she performed cell-based screening of peptides and fragment-based screening by NMR spectroscopy for influenza entry inhibitors, and at the University of Minnesota with Dr. Jon Hawkinson, where she developed and validated biophysical and biochemical assays for

compound characterization and high-throughput screening (HTS), with a special focus on surface plasmon resonance. She is now a permanent research scientist in the HTS lab.

William D. Brubaker is a senior research engineer in the Sensing and Diagnostic Laboratory (SDL) at SRI International. He received his Bachelor of Science in Biomedical Engineering from UC Davis and his Ph.D. in Biological Sciences from UC Irvine. At UC Irvine he worked with Prof. Rachel Martin to determine the molecular structures of human γ S-crystallin and a cataract-related variant. His postdoctoral research was done in the lab of Joe Rogers at SRI International on the interaction between β -amyloid and the innate immune system. He is currently the head of consumable development for several point-of-care medical diagnostic tests being developed at SRI.

Rachel W. Martin is a Professor of Chemistry and Molecular Biology and Biochemistry at UC Irvine. She earned her Bachelor of Science in Chemistry at Arizona State University and her Ph.D. in Chemistry at Yale University in the group of Prof. Kurt Zilm. In her thesis work, she designed and built magic-angle-spinning probes and developed sample preparation methods for high-resolution solid-state NMR spectroscopy of proteins. She performed her postdoctoral research in the group of Prof. Alex Pines at UC Berkeley, where she studied liquid crystals, built one-sided magnets, and pushed the limits of NMR spectroscopy in inhomogeneous fields. She joined the faculty at UC Irvine in 2005. Her current research interests include NMR instrumentation and methodology, structure and function of the crystallin proteins, and enzyme discovery from genomic data.

ACKNOWLEDGMENTS

The Martin laboratory's work on crystallin proteins is supported by NIH Grants 2R01EY021514 to R.W.M and 1R01EY025328 to R.W.M. and D. J. Tobias. Optical spectroscopy data were collected in the UCI Laser Spectroscopy Laboratories under the management of D. Fishman. K.W.R. was supported by NSF Training Grant DGE-1633631 and DMS-1361425 to R.W.M. and C. T. Butts. R.W.M. is a CIFAR Fellow.

REFERENCES

- (1) Horwitz, J.; Bova, M. P.; Ding, L.-L.; Haley, D. A.; Stewart, P. L. Lens α -Crystallin: function and structure. *Eye* **1999**, *13*, 403–408.
- (2) Kosinski-Collins, M. S.; Flaugh, S. L.; King, J. Probing folding and fluorescence quenching in human γD Crystallin Greek key domains using triple tryptophan mutant proteins. *Protein Sci.* **2004**, 13, 2223–2235.
- (3) Chen, J.; Callis, P. R.; King, J. Mechanism of the very efficient quenching of tryptophan fluorescence in human γ D-and γ S-crystallins: the γ -Crystallin fold may have evolved to protect tryptophan residues from ultraviolet photodamage. *Biochemistry* **2009**, *48*, 3708–3716.
- (4) Schafheimer, N.; King, J. Tryptophan cluster protects human γ D-Crystallin from ultraviolet radiation-induced photoaggregation in vitro. *Photochem. Photobiol.* **2013**, *89*, 1106–1115.
- (5) Bova, L. M.; Wood, A. M.; Jamie, J. F.; Truscott, R. J. W. UV filter compounds in human lenses: The origin of 4-(2-amino-3-hydroxyphenyl)-4-oxobutanoic acid O- β -D-glucoside. *Invest. Ophthalmol. Visual Sci.* **1999**, 40, 3237–3244.
- (6) Parker, N. R.; Jamie, J. F.; Davies, M. J.; Truscott, R. J. W. Protein-bound kynurenine is a photosensitizer of oxidative damage. *Free Radical Biol. Med.* **2004**, *37*, 1479–1489.
- (7) Iwami, K.; Wang, J.-Y.; Jain, R.; McCormack, S.; Johnson, L. Intestinal ornithine decarboxylase: half-life and regulation by putrescine. *Am. J. Physiol. Gastrointest. Liver Physiol.* **1990**, 258, G308–G315.

- (8) Mankarious, S.; Lee, M.; Fischer, S.; Pyun, K. H.; Ochs, H. D.; Oxelius, V. A.; Wedgwood, R. J. The half-lives of IgG subclasses and specific antibodies in patients with primary immunode ciency who are receiving intravenously administered immunoglobulin. *J. Lab. Clin. Med.* 1988, 112, 634–640.
- (9) Liu, P.; Edassery, S. L.; Ali, L.; Thomson, B. R.; Savas, J. N.; Jin, J. Long-lived metabolic enzymes in the crystalline lens identified by pulse-labeling of mice and mass spectrometry. *eLife* **2019**, 8, No. e50170.
- (10) Toyama, B. H.; Hetzer, M. W. Protein homeostasis: Live long, won't prosper. *Nat. Rev. Mol. Cell Biol.* **2013**, *14*, 55–61.
- (11) Tardieu, A.; Vérétout, F.; Krop, B.; Slingsby, C. Protein interactions in the calf eye lens: interactions between β -crystallins are repulsive whereas in γ -crystallins they are attractive. *Eur. Biophys. J.* **1992**, 21, 1–12.
- (12) World Health Organization. *Priority Eye Diseases*, 2020. https://www.who.int/blindness/causes/priority/en/index1.html.
- (13) Braun, N.; Zacharias, M.; Peschek, J.; Kastenmüller, A.; Zou, J.; Hanzlik, M.; Haslbeck, M.; Rappsilber, J.; Buchner, S.; Weinkauf, S. Johannesand Weinkauf Multiple molecular architectures of the eye lens chaperone αB-Crystallin elucidated by a triple hybrid approach. *Proc. Natl. Acad. Sci. U. S. A.* **2011**, *108*, 20491–20496.
- (14) Nalini, V.; Bax, B.; Driessen, H.; Moss, D.; Lindley, P.; Slingsby, C. Close packing of an oligomeric eye lens beta-Crystallin induces loss of symmetry and ordering of sequence extensions. *J. Mol. Biol.* **1994**, 236, 1250–1258.
- (15) Wu, Z.; Delaglio, F.; Wyatt, K.; Wistow, G.; Bax, A. Solution structure of γ S-Crystallin by molecular fragment replacement NMR. *Protein Sci.* **2005**, *14*, 3101–3114.
- (16) de Jong, W. W.; Leunissen, J. A.; Voorter, C. E. Evolution of the α -Crystallin/small heat-shock protein family. *Mol. Biol. Evol.* **1993**, *10*, 103-126.
- (17) Aquilina, J. A.; Benesch, J. L. P.; Bateman, O. A.; Slingsby, C.; Robinson, C. V. Polydispersity of a mammalian chaperone: Mass spectrometry reveals the population of oligomers in α B-Crystallin. *Proc. Natl. Acad. Sci. U. S. A.* **2003**, *100*, 10611–10616.
- (18) Jehle, S.; Rajagopal, P.; Bardiaux, B.; Markovic, S.; Kuhne, R.; Stout, J.; Higman, V.; Klevit, R.; van Rossum, B.; Oschkinat, H. Solidstate NMR and SAXS studies provide a structural basis for the activation of α B-Crystallin oligomers. *Nat. Struct. Mol. Biol.* **2010**, *17*, 1037–1042
- (19) Delbecq, S. P.; Klevit, R. E. One size does not fit all: the oligomeric states of α B-Crystallin. *FEBS Lett.* **2013**, *587*, 1073–1080.
- (20) Kaiser, C. J.; Peters, C.; Schmid, P. W.; Stavropoulou, M.; Zou, J.; Dahiya, V.; Mymrikov, E. V.; Rockel, B.; Asami, S.; Haslbeck, M.; Rappsilber, J.; Reif, B.; Zacharias, M.; Buchner, J.; Weinkauf, S. The structure and oxidation of the eye lens chaperone α A-Crystallin. *Nat. Struct. Mol. Biol.* **2019**, *26*, 1141–1150.
- (21) Sharma, K. K.; Kumar, R. S.; Kumar, G. S.; Quinn, P. T. Synthesis and characterization of a peptide identified as a functional element in α -Crystallin. *J. Biol. Chem.* **2000**, *275*, 3767–3771.
- (22) Srivastava, S. S.; Mishra, A.; Krishnan, B.; Sharma, Y. Ca²⁺-binding motif of $\beta\gamma$ -crystallins. *J. Biol. Chem.* **2014**, 289, 10958–10966
- (23) Kong, F.; King, J. Contributions of aromatic pairs to the folding and stability of long-lived human γ D-Crystallin. *Protein Sci.* **2011**, *20*, 513–528.
- (24) Mills, I. A.; Flaugh, S. L.; Kosinski-Collins, M. S.; King, J. A. Folding and stability of the isolated Greek key domains of the long-lived human lens proteins γ D-Crystallin and γ S-Crystallin. *Protein Sci.* **2007**, *16*, 2427–2444.
- (25) Sun, H.; Ma, Z.; Li, Y.; Liu, B.; Li, Z.; Ding, X.; Gao, Y.; Ma, W.; Tang, X.; Li, X.; Shen, Y. Gamma-S Crystallin gene (CRYGS) mutation causes dominant progressive cortical cataract in humans. *J. Med. Genet.* **2005**, 42, 706–710.
- (26) Brubaker, W. D.; Freites, J. A.; Golchert, K. J.; Shapiro, R. A.; Morikis, V.; Tobias, D. J.; Martin, R. W. Separating instability from aggregation propensity in γ S-Crystallin variants. *Biophys. J.* **2011**, *100*, 498–506.

- (27) Brubaker, W. D.; Martin, R. W. 1 H, 13 C, and 15 N assignments of wild-type human γ S-Crystallin and its cataract-related variant γ S-G18V. *Biomol. NMR Assignments* **2012**, *6*, 63–67.
- (28) Jiang, J.; Golchert, K. J.; Kingsley, C. N.; Brubaker, W. D.; Martin, R.; Mukamel, S. Exploring the aggregation propensity of γ S-Crystallin protein variants using two-dimensional spectroscopic tools. *J. Phys. Chem. B* **2013**, *117*, 14294–14301.
- (29) Forsythe, H. M.; Vetter, C. J.; Jara, K. A.; Reardon, P. N.; David, L. L.; Barbar, E. J.; Lampi, K. J. Altered protein dynamics and increased aggregation of human γScrystallin due to cataract-associated deamidations. *Biochemistry* **2019**, *58*, 4112–4124.
- (30) Kingsley, C. N.; Brubaker, W. D.; Markovic, S.; Diehl, A.; Brindley, A. J.; Oschkinat, H.; Martin, R. W. Preferential and specific binding of human α B-Crystallin to a cataract-related variant of γ S-Crystallin. *Structure* **2013**, *21*, 2221–2227.
- (31) Serebryany, E.; Woodard, J. C.; Adkar, B. V.; Shabab, M.; King, J. A.; Shakhnovich, E. I. An internal disulfide locks a misfolded aggregation-prone intermediate in cataract-linked mutants of human γD-Crystallin. *J. Biol. Chem.* **2016**, *291*, 19172–19183.
- (32) Thorn, D. C.; Grosas, A. B.; Mabbitt, P. D.; Ray, N. J.; Jackson, C. J.; Carver, J. A. The structure and stability of the disulfide-linked γS-Crystallin dimer provide insight into oxidation products associated with lens cataract formation. *J. Mol. Biol.* **2019**, 431, 483–497.
- (33) Boatz, J. C.; Whitley, M. J.; Li, M.; Gronenborn, A. M.; van der Wel, P. C. Cataract-associated P23T γ D-Crystallin retains a native-like fold in amorphous-looking aggregates formed at physiological pH. *Nat. Commun.* **2017**, *8*, 15137.
- (34) Kingsley, C. N.; Bierma, J. C.; Pham, V.; Martin, R. The γ S-Crystallin proteins from the Antarctic nototheniid toothfish: a model system for investigating differential resistance to chemical and thermal denaturation. *J. Phys. Chem. B* **2014**, *118*, 13544–13553.
- (35) Martin, R. W. NMR studies of eye lens crystallins. *eMagRes* **2014**, 3 (2), 139–152.
- (36) Sprague-Piercy, M. A.; Roskamp, K. W.; Wong, E.; Fakhoury, J. N.; Freites, J. A.; Tobias, D. J.; Martin, R. Human α B-Crystallin discriminates between aggregation-prone and function-preserving variants of a client protein. *Biochim. Biophys. Acta, Gen. Subj.* **2020**, 1864, 129502.
- (37) Khago, D.; Wong, E. K.; Kingsley, C. N.; Freites, J. A.; Tobias, D. J.; Martin, R. W. Increased hydrophobic surface exposure in the cataract-related G18V variant of human γS-Crystallin. *Biochim. Biophys. Acta, Gen. Subj.* **2016**, *1860*, 325–332.
- (38) Armstrong, B. D.; Han, S. A new model for Overhauser enhanced nuclear magnetic resonance using nitroxide radicals. *J. Chem. Phys.* **2007**, *127*, 104508.
- (39) Huang, K.-Y.; Kingsley, C. N.; Sheil, R.; Cheng, C.-Y.; Bierma, J. C.; Roskamp, K. W.; Khago, D.; Martin, R. W.; Han, S. Stability of protein-specific hydration shell on crowding. *J. Am. Chem. Soc.* **2016**, 138, 5392–5402.
- (40) Zhang, T. O.; Alperstein, A. M.; Zanni, M. T. Amyloid β -sheet secondary structure identified in UV-induced cataracts of porcine lenses using 2D IR spectroscopy. *J. Mol. Biol.* **2017**, *429*, 1705–1721.
- (41) Roskamp, K. W.; Montelongo, D. M.; Anorma, C. D.; Bandak, D. N.; Chua, J. A.; Malecha, K. T.; Martin, R. W. Multiple aggregation pathways in human γ S-Crystallin and Its aggregation-prone G18V variant. *Invest. Ophthalmol. Visual Sci.* **2017**, *58*, 2397–2405.
- (42) Das, P.; King, J. A.; Zhou, R. Aggregation of γ -crystallins associated with human cataracts via domain swapping at the C-terminal β -strands. *Proc. Natl. Acad. Sci. U. S. A.* **2011**, *108*, 10514–10519.
- (43) Serebryany, E.; King, J. A. Wild-type human γ D-Crystallin promotes aggregation of Its oxidation-mimicking, misfolding-prone W42Q mutant. *J. Biol. Chem.* **2015**, 290, 11491–11503.
- (44) Wong, E. K.; Prytkova, V.; Freites, J. A.; Butts, C. T.; Tobias, D. J. Molecular mechanism of aggregation of the cataract-related γ D-Crystallin W42R variant from multiscale atomistic simulations. *Biochemistry* **2019**, *58*, 3691–3699.

Accounts of Chemical Research

- (45) Mahler, B.; Chen, Y.; Ford, J.; Thiel, C.; Wistow, G.; Wu, Z. Structure and dynamics of the fish eye lens protein, γ M7-Crystallin. *Biochemistry* **2013**, *52*, 3579–3587.
- (46) Whitley, M.; Xi, Z.; Bartko, J.; Jensen, M.; Blackledge, M.; Gronenborn, A. A combined NMR and SAXS analysis of the partially folded cataract-associated V75D γ D-Crystallin. *Biophys. J.* **2017**, *112*, 1135–1146.
- (47) Domínguez-Calva, J. A.; Pérez-Vázquez, M. L.; Serebryany, E.; King, J. A.; Quintanar, L. Mercury-induced aggregation of human lens γ-crystallins reveals a potential role in cataract disease. *JBIC*, *J. Biol. Inorg. Chem.* **2018**, 23, 1105–1118.
- (48) Quintanar, L.; Domínguez-Calva, J. A.; Serebryany, E.; Rivillas-Acevedo, L.; Haase-Pettingell, C.; Amero, C.; King, J. A. Copper and zinc ions specifically promote nonamyloid aggregation of the highly stable human γD-Crystallin. ACS Chem. Biol. 2016, 11, 263–272.
- (49) Shimeld, S. M.; Purkiss, A. G.; Dirks, R. P.; Bateman, O. A.; Slingsby, C.; Lubsen, N. H. Urochordate $\beta\gamma$ -Crystallin and the evolutionary origin of the vertebrate eye lens. *Curr. Biol.* **2005**, *15*, 1684–1689.
- (50) Mishra, A.; Krishnan, B.; Srivastava, S. S.; Sharma, Y. Microbial $\beta\gamma$ -crystallins. *Prog. Biophys. Mol. Biol.* **2014**, *115*, 42–51.
- (51) Kozlyuk, N.; Sengupta, S.; Bierma, J. C.; Martin, R. Calcium binding dramatically stabilizes an ancestral Crystallin fold in tunicate $\beta\gamma$ -Crystallin. *Biochemistry* **2016**, *55*, 6961–6968.
- (52) Roskamp, K. W.; Kozlyuk, N.; Sengupta, S.; Bierma, J. C.; Martin, R. W. Divalent cations and the divergence of $\beta\gamma$ -crystallin function. *Biochemistry* **2019**, *58*, 4505–4518.
- (53) Suman, S. K.; Mishra, A.; Yeramala, L.; Rastogi, I. D.; Sharma, Y. Disability for function: loss of Ca²⁺-binding is obligatory for fitness of mammalian $\beta \gamma$ -crystallins. *Biochemistry* **2013**, *52*, 9047–9058.
- (54) Jobby, M. K.; Sharma, Y. Calcium-binding to lens β B2-and β A3-crystallins suggests that all β -crystallins are calcium-binding proteins. *FEBS J.* **2007**, *274*, 4135–4147.
- (55) Rajini, B.; Shridas, P.; Sundari, C. S.; Muralidhar, D.; Chandani, S.; Thomas, F.; Sharma, Y. Calcium binding properties of γ -Crystallin: calcium ion binds at the Greek key β γ -Crystallin fold. *J. Biol. Chem.* **2001**, 276, 38464–38471.
- (56) Zhao, H.; Brown, P. H.; Schuck, P. On the distribution of protein refractive index increments. *Biophys. J.* **2011**, *100*, 2309–2317.
- (57) Khago, D.; Bierma, J. C.; Roskamp, K. W.; Kozlyuk, N.; Martin, R. Protein refractive index increment is determined by conformation as well as composition. *J. Phys.: Condens. Matter* **2018**, *30*, 435101.
- (58) Zhao, H.; Chen, Y.; Rezabkova, L.; Wu, Z.; Wistow, G.; Schuck, P. Solution properties of γ-crystallins: Hydration of fish and mammal γ-crystallins. *Protein Sci.* **2014**, 23, 88–99.
- (59) Grishaev, A.; Wu, J.; Trewhella, J.; Bax, A. Refinement of multidomain protein structures by combination of solution small-angle x-ray scattering and NMR data. *J. Am. Chem. Soc.* **2005**, 127, 16621–16628.
- (60) Wang, J.; Zuo, X.; Yu, P.; Byeon, I.; Jung, J.; Wang, X.; Dyba, M.; Seifert, S.; Schwieters, C.; Qin, J.; Gronenborn, A.; Wang, Y. Determination of multicomponent protein structures in solution using global orientation and shape restraints. *J. Am. Chem. Soc.* **2009**, *131*, 10507–10515.